Materials Science Forum
ISSN: 1662-9752, Vol. 1062, pp 3-7
doi:10.4028/p-9bg88x

Submitted: 2021-09-21
Revised: 2022-02-01
Accepted: 2022-02-08
Online: 2022-05-31

Models for Impurity Incorporation during Vapor-Phase Epitaxy

Kazuhiro Mochizuki[1,a*], Fumimasa Horikiri[2,b] , Hiroshi Ohta[1,c] and Tomoyoshi Mishima[1,d]

[1]Hosei University, Koganei, Tokyo 184-8584, Japan

[2]SCIOCS Co. Ltd., Hitachi, Ibaraki 319-1418, Japan

[a]kazuhiro.mochizuki.66@hosei.ac.jp, [b]horikirif@sc.sumitomo-chem.co.jp, [c]hiroshi.ohta.43@hosei.ac.jp, [d]tomoyoshi.mishima.67@hosei.ac.jp

Keywords: impurity, vapor-phase epitaxy, surface diffusion, step kinetics, segregation.

Abstract. Impurity incorporation during vapor-phase epitaxy on stepped surfaces was modeled by classifying rate-limiting processes into i) surface diffusion, ii) step kinetics, and iii) segregation. Examples were shown for i) desorption-limited Al incorporation during chemical vapor deposition (CVD) of (0001) SiC, ii) preferential desorption of C atoms from kinks during CVD of Al-doped (000-1) SiC, and iii) segregation-limited C incorporation during metalorganic vapor-phase epitaxy of (0001), (000-1), and (10-10) GaN.

Introduction

Impurity incorporation during vapor-phase epitaxy has been modeled via, for example, site competition [1,2] and surface vacancies [3,4]. The latter, however, cannot explain the variation in impurity doping around facets [5]. Moreover, in the cases of homoepitaxial growths of SiC and GaN, misoriented substrates are often used for polytype [6] and doping-uniformity [7] controls, respectively. Accordingly, we modeled impurity incorporation during step-flow growth by taking Al-doped SiC and C-doped GaN, as examples. We believe the models should be beneficial for determining allowable off-angle variations for desired doping-level uniformities in advanced devices. Although Al was chosen due to the availability of a thermodynamic model [8], N doping for SiC could be similarly treated under the assumption of the N segregation coefficient being unity [9].

Proposed Models

Impurity incorporation during vapor-phase epitaxy on stepped surfaces was modeled by classifying rate-limiting processes into i) surface diffusion [10], ii) step kinetics [11], and iii) segregation [12] (Table I).

i) **Desorption** limits impurity incorporation at step-edges when surface diffusion length λ is less than a half of the average inter-step distance, λ_o. This should be the case with incorporation of Al, whose λ was estimated to be less than 2 nm at 1550°C [10], into stepped 4H-SiC (0001). This is due to relatively large λ_o (eg., 7.2 nm for $\theta = 8°$) originating from four-bilayer-high steps [13]. Based on the Burton−Cabrera−Frank (BCF) theory [14], we derived the following equation for x in $Al_xSi_{1-x}C$ [10]:

$$F_{Al} / x = [\gamma P_{Si}^{e} / K (2 \pi m_{Al} k_B T_g)^{1/2}] + [F_{Si} - P_{Si}^{e} / (2 \pi m_{Si} k_B T_g)^{1/2}] [\lambda_o / 2\lambda_{Al} \tanh (\lambda_o / 2\lambda_{Al})], \quad (1)$$

where F_i, P_i^e, and m_i (i = Al, Si) are, respectively, the incident flux, equilibrium vapor pressure, and mass of i atom, K and γ are, repectively, the equilibrium constant and activity coefficient for AlC, T_g is growth temperature, and k_B is Boltzmann's constant. Eq. (1) explains why x was independent of the off-angle θ (ranging from 2° to 8°) when the C/Si ratio, r, was small (i.e., 1.8 [15]); due to large P_{Si}^e, the first term in the right-hand side, which corresponds to the Al desorption flux, became

dominant (solid line in Fig. 1). Eq. (1) also explains why x increased with θ when r was large (i.e., 4−6 [16]); due to small P_{Si}^{e}, the second term in the right-hand side, which corresponds to the Al flux incorporated into the solid, became so large that x increased with the step density on the surface (dashed and dotted lines in Fig. 1).

Table I. Rate-limiting processes of impurity incorporation during vapor-phase epitaxy.

Classification of host-atom desorption from kinks	Surface-diffusion length of impurity atoms	
	Less than $\lambda_o/2$	Much larger than $\lambda_o/2$
Preferential desorption of host atoms from kinks	Surface diffusion	Step kinetics
Negligible desorption of host atoms from kinks		Segregation

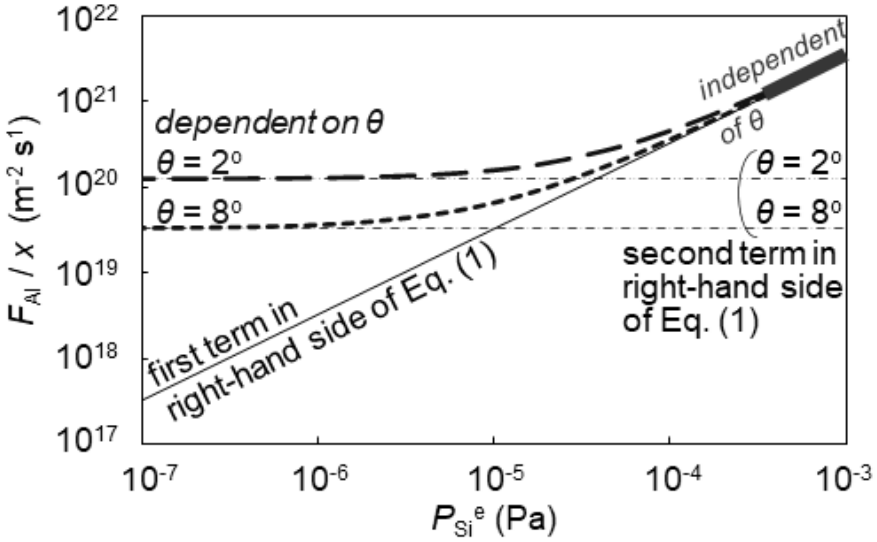

Fig. 1. F_{Al}/x, calculated as first term (solid line) and second term (dashed and dotted lines) in right-hand side of Eq. (1), as a function of equilibrium vapor pressure of Si, with assumptions of T_g of 1550ºC, growth rate of 1.3 μm/h, and λ_{Al} of 2.0 nm.

ii) Preferential desorption of host atoms from kinks limits impurity incorporation at kinks even when $\lambda >> \lambda_o/2$. This should be the case with incorporation of Al into 4H-SiC (000-1) that has one-bilayer-high steps [13]. We assume that a C atom making two bonds with a Si atom stays at kinks, while that a C atom making one bond with a Si atom easily desorbs from kinks [Fig. 2(a)].

Since r is typically small (eg., $r \leq 6$ [16]), some surface-diffusing Al atoms that arrive at kinks keep waiting (for an average time τ_C) until C atoms make one bond with Si atoms at kinks [Fig. 2(b)] before they are incorporated into the solid [Fig. 2(c)]. Based on the reported experimental results [16], surface Al concentration n_{Al} (normalized by the mean residence time τ_{Al}) was calculated (Fig. 3). n_{Al} in the vicinity of step-edges (i.e., local minima in Fig. 3) on (000-1) is much larger than that on (0001), indicating longer τ_C on (000-1).

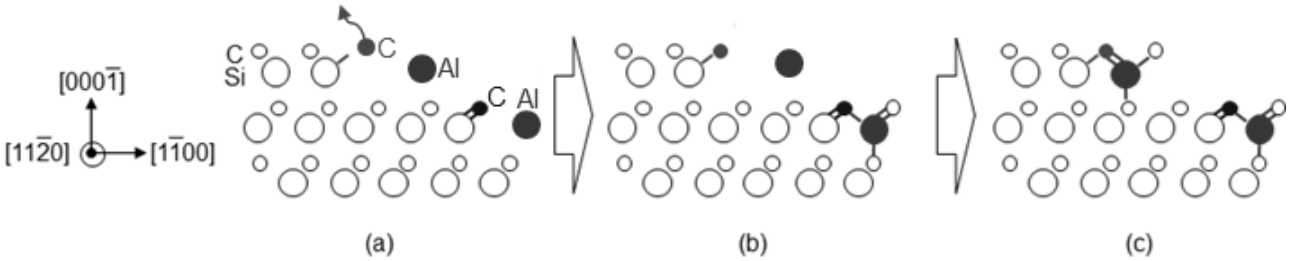

Fig. 2. Schematic illustrations of (a) preferential desorption of a C atom having one bond with a Si atom, (b) adsorption of a C atom to a dangling bond of a Si atom and bonding of an Al atom to two C atoms, and (c) bonding of another Al atom to three C atoms at kinks on 4H-SiC (000-1).

iii) Segregation limits impurity incorporation even when $\lambda >> \lambda_o/2$ and desorption of host atoms from kinks is negligible. This should be the case with incorporation of C into GaN that is typically grown with the N/Ga ratio exceeding 1000 [17−19]; namely, soon after a N atom making one bond with a Ga atom desorbs from kinks, another N atom makes one bond with the Ga atom. When the length of time before the C concentration at the step-edge site reaches its equilibrium value, τ_{step}, is much smaller than the meantime until a C atom incorporated at kinks moves through the step-edge site to the surface site, τ, the C concentration in the solid can be expressed as [20]

$$N = N_{surf} + (N_{step} - N_{surf}) \exp(-D / V_{step}\, a), \tag{2}$$

where N_{surf} and N_{step} are, respectively, the equilibrium C concentrations at the surface site and at the step-edge site, D is the diffusion coefficient in the solid, V_{step} is the average step velocity, and a is the lattice constant. As shown in Fig. 4, the results for (0001) [17], (000-1) [18], and (10-10) [19] growths are well reproduced with D of 2×10^{-13} cm^2/s that agrees with the experimentally determined value [21].

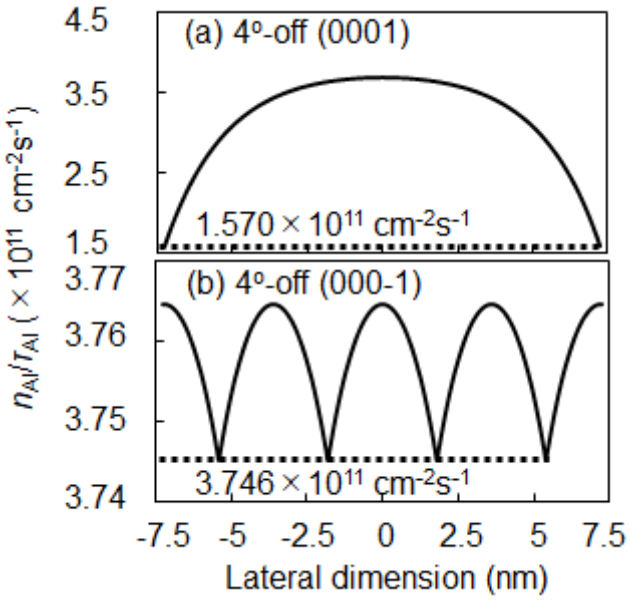

Fig. 3. Distribution of n_{Al}/τ_{Al} calculated with assumptions of T_g of 1550°C, growth rate of 1.3 μm/h, r of 6, and λ_{Al} of 2.0 nm.

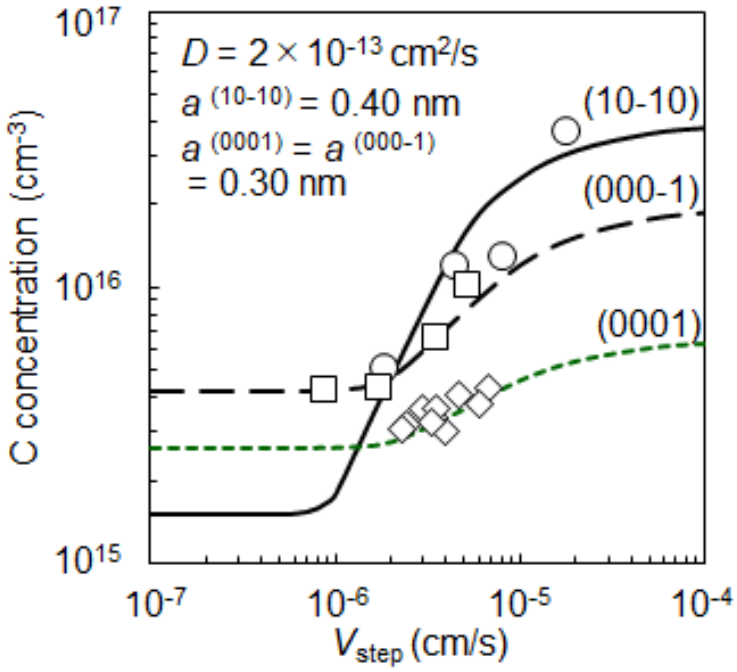

Fig. 4. Step-velocity dependences of carbon concentrations fitted to the reported results [17−19].

Summary

Impurity incorporation during step-flow growth was modeled and exemplified by SiC: Al and GaN: C cases. We believe the proposed models should contribute to determining allowable off-angle variations for desired doping-level uniformities in advanced SiC and GaN devices.

Acknowledgments

This work was supported in part by the "Project of GaN technology innovation for enabling decarbonized society and lifestyle" funded by the Ministry of the Environment Government of Japan.

References

[1] D.J. Larkin, P.G. Neudeck, J.A. Powell and L. G. Matus, Appl. Phys. Lett. 65 (1994) 1659−1661.

[2] R. Wang and A.J. Steckl, J. Cryst. Growth 312 (2010) 680−684.

[3] G. Ferro and D. Chaussende, Sci. Rep. 7 (2017) 43069-1−43069-11.

[4] G. Ferro, D. Chaussende and N. Tsavdaris, J. Cryst. Growth 507 (2019) 338−343.

[5] K. Yokomoto, M. Yabu, T. Hashiguchi and N. Ohtani, J. Appl. Phys. 128 (2020) 135701-1−135701-9.

[6] N. Kuroda, K. Shibahara, W. S. Yoo, S. Nishino and H. Matsunami, Ext. Abstr. 19th Conf. Solid State Devices & Materials, 1987, 227−229.

[7] F. Horikiri, Y. Narita, T. Yoshida, T. Kitamura, H. Ohta, T. Nakamura and T. Mishima, IEEE Trans. Semicond. Manufact. 30 (2017) 486−492.

[8] A.S. Segal, S.Yu. Karpov, A.V. Lobanova, E.V. Yakovlev, K. Hara and M. Naito, Mater. Sci. Forum 821−823 (2015) 145−148.

[9] K. Mochizuki and T. Mishima, Jpn. J. Appl. Phys. 60 (2021) 018001-1−018001-3.

[10] K. Mochizuki and T. Mishima, Jpn. J. Appl. Phys. 59 (2020) 088003-1−088003-4.

[11] K. Mochizuki, F. Horikiri, H. Ohta and T. Mishima, Jpn. J. Appl. Phys 59 (2020) 068001-1−068001-3.

[12] K. Mochizuki, F. Horikiri, H. Ohta and T. Mishima, Jpn. J. Appl. Phys 60 (2021) 018002-1−018002-3.

[13] T. Kimoto, A. Itoh, H. Matsunami and T. Okano, J. Appl. Phys. 81 (1997) 3494−3500.

[14] W.K. Burton, N. Cabrera, and F.C. Frank, Philos. Trans. R. Soc. London, Ser. A 243 (1951) 299-358.

[15] Information on https://tel.archives-ouvertes.fr/tel-01466713/document

[16] T. Yamamoto, T. Kimoto and H. Matsunami, Mater. Sci. Forum 264−268 (1998) 111−114.

[17] F. Horikiri, Y. Narita, T. Yoshida, T. Kitamura, H. Ohta, T. Nakamura and T. Mishima, Jpn. J. Appl. Phys. 56 (2017) 061001-1−061001-6.

[18] K. Nagamatsu, Y. Ando, T. Kono, H. Cheong, S. Nitta, Y. Honda, M. Pristovsek and H. Amano, J. Cryst. Growth 512 (2019) 78−83.

[19] H. Yamada, H. Chonan, T. Takahashi and M. Shimizu, Jpn. J. Appl. Phys. 57 (2018) 04FG01-1−04FG01-5.

[20] T. Nishinaga, C. Sasaoka and K. Park, Jpn. J. Appl. Phys 28 (1989) 836−840.

[21] X.A. Cao, R.G. Wilson, J.C. Zolper, S.J. Pearton, J. Han, R.J. Shul, D.J. Rieger, R.K. Singh, M. Fu, V. Scarvepalli, J.A. Sekhar and J.M. Zavada, J. Electron. Mater. 28 (1999) 261-265.